

## RESEARCH ARTICLE | *The Physiology of Immune Therapies and Their Application in Treating Gastrointestinal Cancers*

# Vaccine against gastrin, a polyclonal antibody stimulator, decreases pancreatic cancer metastases

Nicholas Osborne,<sup>1</sup> Rebecca Sundseth,<sup>1</sup> Martha D. Gay,<sup>2</sup> Hong Cao,<sup>2</sup> Robin D. Tucker,<sup>3</sup> Sandeep Nadella,<sup>2</sup> Shangzi Wang,<sup>4</sup> Xunxian Liu,<sup>5</sup> Alexander Kroemer,<sup>5</sup> Lynda Sutton,<sup>6</sup> Allen Cato,<sup>6</sup> and  Jill P. Smith<sup>2</sup>

<sup>1</sup>Cato Research, Durham, North Carolina; <sup>2</sup>Department of Medicine, Georgetown University, Washington, District of Columbia; <sup>3</sup>Department of Pathology, Georgetown University, Washington, District of Columbia; <sup>4</sup>Department of Oncology, Georgetown University, Washington, District of Columbia; <sup>5</sup>The MedStar Georgetown Transplant Institute, Georgetown University, Washington, District of Columbia; and <sup>6</sup>Cancer Advances, Durham, North Carolina

Submitted 30 May 2019; accepted in final form 5 August 2019

**Osborne N, Sundseth R, Gay MD, Cao H, Tucker RD, Nadella S, Wang S, Liu X, Kroemer A, Sutton L, Cato A, Smith JP.** Vaccine against gastrin, a polyclonal antibody stimulator, decreases pancreatic cancer metastases. *Am J Physiol Gastrointest Liver Physiol* 317: G682–G693, 2019. First published August 21, 2019; doi: 10.1152/ajpgi.00145.2019.—Growth of pancreatic cancer is stimulated by gastrin in both a paracrine and an autocrine fashion. Traditional therapies have not significantly improved survival, and recently pancreatic cancer has been deemed a “cold” tumor due to its poor response to immunotherapy. Strategies to improve survival of pancreatic cancer are desperately needed. In the current investigation, we studied the effects of an anti-gastrin cancer vaccine, polyclonal antibody stimulator (PAS; formerly called G17DT and Gastrimmune), used alone or in combination with a programmed cell death receptor (PD)-1 immune checkpoint antibody on pancreatic cancer growth, metastases, and the tumor microenvironment (TME). Immune-competent female C57BL/6 mice bearing syngeneic orthotopic murine pancreatic cancer treated with PAS had significantly smaller tumors and fewer metastases. Examination of the TME demonstrated decreased fibrosis with fewer M2 and more M1 tumor-associated macrophages. Expression of the *E-cadherin* gene was significantly increased and expression of the *TGFβR2* gene was decreased compared with controls. Mice treated with PAS or the combination of PAS and PD-1 antibody exhibited significantly less tumor expression of phospho-paxillin, the focal adhesion protein β-catenin, and matrix metalloproteinase-7. This study suggests that inhibition of the cancer-promoting effects of gastrin in pancreatic cancer can decrease metastases by altering the TME and decreasing pathways that activate the epithelial mesenchymal transition. The PAS vaccine appears to change the TME, making it more susceptible to therapy with an immune checkpoint antibody. This novel combination of two immunotherapies may improve survival of pancreatic cancer by decreasing both tumor growth and metastasis formation.

**NEW & NOTEWORTHY** Survival from advanced pancreatic cancer is poor, in part due to dense fibrosis of the tumor microenvironment, increased number of M2-polarized macrophages that promote angiogenesis and invasion, and lack of “target-specific” therapy. Herein, we report that a tumor vaccine that selectively targets gastrin decreases pancreatic cancer growth and metastases. Furthermore, the gastrin vaccine polyclonal antibody stimulator alters the tumor mi-

croenvironment rendering it more responsive to immunotherapy with a programmed cell death receptor-1 immune checkpoint antibody.

epithelial mesenchymal transition; gastrin; tumor-associated macrophages; tumor immunology; tumor microenvironment

## INTRODUCTION

A predominant feature of pancreatic cancer is its propensity to metastasize early and frequently (64). In fact, 90% of patients have advanced disease at the time of presentation (9). Although the retroperitoneal location and nonspecific symptoms may contribute to late stage diagnosis of pancreatic cancer, some characteristic features associated with this malignancy may facilitate metastases. One of the first steps in the metastatic cascade is invasion, a process that involves the loss of cell-cell adhesion and changes in the extracellular matrix to promote motility and migration (24). Epithelial-cadherin (E-cadherin) is a major component in the adherens junctions and is responsible for maintaining the epithelial cell phenotype (25, 52, 54). β-Catenin is involved in cell-cell adhesion through interaction with the E-cadherin cell-adhesion complex and the microtubule network (34). Activation of the Wnt/β-catenin pathway with overexpression of β-catenin is found in pancreatic cancer (67). Paxillin is a focal adhesion protein that functions by recruiting structural and signaling molecules involved in cell motility and migration (22). When paxillin interacts with integrins from the extracellular matrix, it becomes phosphorylated and it provides a scaffold for the recruitment of tyrosine kinases FAK and Src (22). Primary cancer cells undergo a transformational process called epithelial-mesenchymal transition (EMT) (20) that is regulated by a network of cytokines, transcription factors, growth factors, and signaling pathways in the tumor microenvironment (TME) that leads to metastasis (57). EMT can be induced by the activation of the transforming growth factor-β (TGF-β) signaling pathway to promote metastasis (5), and cancer epithelial cell and immune cells interactions are mediated by TGF-β.

Immune cells of the tumor microenvironment also play a role in promoting cancer invasion and metastases. The pancreatic TME is characterized by a lack of tumor-infiltrating lymphocytes and an abundance of tumor-associated macro-

Address for reprint requests and other correspondence: J. P. Smith, Georgetown Univ., 4000 Reservoir Rd., NW, Bldg. D, Room 338, Washington, DC 20007 (e-mail: jps261@georgetown.edu).

phages (TAMs) (39). Rather than promoting tumor killing, these immune cells promote tumor growth and invasion (55, 68). TAMs can polarize to be either tumor killing (M1) or tumor promoting (M2) (38). The polarization of macrophages is identified by expression of processing enzymes: nitric oxide synthase is associated with M1 proinflammatory TAMs and arginase I (ARGI) expression is associated with M2, tumor-promoting TAMs (6). The pancreatic TME has an abundance of M2 polarized or tumor-promoting macrophages (36, 68), and this macrophage population overexpresses programmed cell death receptor-1 (PD-1) that further impairs the phagocytic potency of these TAMs (16). Tumors recruit macrophages that suppress immune functions and promote growth and metastases (10). TAMs have been shown to be required for tumor cell migration and invasion (10). Tumor cells secrete colony-stimulating factor-1, which activates TAMs to migrate and produce epidermal growth factor, which then in turn leads to migration and metastasis of tumor cells (62). TAMs also deliver vascular endothelial growth factor (VEGF) to promote angiogenesis, and increased expression of VEGF receptor-1 (VEGFR-1) has been shown to enhance cell migration and invasion in pancreatic cancer (65). Blockade of PD-1/programmed death ligand-1 (PD-L1) binding with immune checkpoint antibodies promotes activity of the TAMs and prolongs survival of tumor-bearing mice (16).

The gastrointestinal peptide gastrin has been shown to stimulate growth of pancreatic cancer in both a paracrine (41) and autocrine (45) fashion. Gastrin has also been shown to increase  $\beta$ -catenin (70) and VEGF-A expression (13) in cancers thus promoting the EMT. We hypothesized that if the actions of gastrin are decreased, then pancreatic cancer growth and metastases will be inhibited. A vaccine to gastrin, formerly termed G17DT and Gastrimmune, and now called polyclonal antibody stimulator (PAS), has been previously studied in gastrointestinal cancers and shown to improve overall survival in patients with pancreatic cancer in whom the vaccine elicited a B-cell response with the generation of anti-gastrin antibodies (15). PAS targets the form of gastrin G17, which has been shown to be overexpressed in, and to stimulate the growth of, pancreatic cancers (41, 43, 45). Recently, in a preclinical subcutaneous murine model of pancreatic cancer, we demonstrated that PAS vaccination also induced a T-cell response and increased the number of tumor-infiltrating lymphocytes. The purpose of this investigation was to determine if PAS therapy could alter the TME of pancreatic cancer and decrease metastases.

## MATERIALS AND METHODS

**Cell line characterization.** The mT3–2D cells (mT3 cells) were a gift from the laboratory of Dr. David Tuveson, Cold Spring Harbor, NY. This murine pancreatic cancer cell line was derived from *Kras*<sup>+/*LSL-G12D*</sup>; *Trp53*<sup>+/*LSL-R172H*</sup>; *Pdx-Cre* (“KPC”) mice and is syngeneic to C57BL/6 mice (7). Tumors formed from the mT3 cells have characteristics similar to human pancreatic cancer including mutant *Kras* and a dense stroma of fibrosis in the TME void of CD8<sup>+</sup> lymphocytes (7). We previously showed these cancer cells are similar to human pancreatic cancers (48) in that they express cholecystokinin (CCK)-B (or CCK2) receptors (51). The mT3 cells were further characterized in this study for CCK-B receptors, PD-L1 receptors, and gastrin peptide expression by RT-PCR or by immunohistochemistry and immunofluorescence. For mRNA expression, total RNA (1  $\mu$ g) was reversely transcribed using a c-DNA synthesis kit (GeneCopoeia). The cDNA was subjected to

RT-PCR in a thermal cycler under the following conditions: initial incubation for 10 min at 95°C followed by 35 cycles of 95°C  $\times$  30 s, 60°C  $\times$  1 min, and 72°C for 30 s, using primers with DNA sequences included in Table 1. Hypoxanthine phosphoribosyl transferase (HPRT) reference gene primers were used for the internal control. PCR products were evaluated by gel electrophoresis in a 2% agarose gel.

CCK-B receptor, PD-L1 receptor, and gastrin peptide immunoreactivity was confirmed with immunohistochemistry or immunofluorescence and confocal microscopy. mT3 cells were reacted with CCK-B receptor antibody (1:200 dilution; ab77077; Abcam, Toronto, Canada) conjugated to Dylight 488 (ab201799). Nuclei were stained with Hoechst: NucBlue (ThermoFisher). Gastrin immunoreactivity was evaluated in mT3 cancer cells by incubation with a polyclonal gastrin antibody (T-4347; 1:1,000 dilution; Peninsula Laboratories, Carlsbad, CA) overnight at 4°C, followed by incubation with a secondary goat anti-rabbit rhodamine-labeled antibody (1:200 dilution; Thermo Scientific) for 1 h at room temperature in the dark. Nuclei were visualized following DAPI staining. Images of cells were taken with a  $\times$ 40 objective on a Zeiss (LSM-510) confocal microscope. To analyze PD-L1 receptor immunoreactivity, mT3 tumor sections (5  $\mu$ m) were made and reacted with a rabbit anti-mouse PD-L1 antibody (titer 1:75 dilution; cat. no. 17952-1-AP; anti-intech) for 1 h and then a secondary horseradish peroxidase (HRP)-rabbit antibody (DAKO; cat. no. K4003; Agilent) for 30 min. Stained cells were visualized following reaction with HRP substrate DAB (cat. no. K346811-2; Agilent).

**Animals and establishment of orthotopic tumors.** All animal studies were performed in an ethical fashion under a protocol approved by the Georgetown University Institutional Animal Care and Use Committee. Forty, 6-wk-old female C57BL/6 mice underwent anesthesia and sterile surgical injection of 100,000 murine mT3 pancreatic cancer cells into the tail-body of each pancreas. The mT3 cells were stably transfected with luciferase to measure tumor growth in this retroperitoneal location. The retroperitoneum and abdominal wall were sutured closed, and animals were allowed 1 wk for recovery and establishment of tumors. At baseline, 1 wk after tumor inoculation, and then weekly, luciferin (30 mg/ml; Nanolight Technology) was administered to mice (using a 27-gauge needle) by intraperitoneal injection at a concentration of 150 mg/kg in a volume of 100  $\mu$ l to measure tumor size and to quantify metastases with the IVIS Lumina

Table 1. Primers for RT-PCR and quantitative RT-PCR

Gene (Murine)/Direction	Primer Sequence (5'→3')
mCCKAR	
Forward	5'-CTTTCTGCCTGGATCAACCT-3'
Reverse	5'-ACCGTGATAACCAGCGTGTTC-3'
mCCKBR	
Forward	5'-GATGGCTGCTACGTGCAACT-3'
Reverse	5'-CGCACCACCCGCTTCTTAG-3'
mGast	
Forward	Per manufacturer (Genocopia)
Reverse	Per manufacturer (Genocopia)
mHPRT	
Forward	5'-TCCTCCTCAGACCGCTTT-3'
Reverse	5'-TTTTCCAAATCCTCGGCATAATG-3'
mCDH1	
Forward	5'-GGTCATCAGTGTGCTCAGCTCT-3'
Reverse	5'-GCTGTTGTGCTCAAGCCTTCAC-3'
mTGFB2	
Forward	5'-TTTCGGAAGAATACACCAC-3'
Reverse	5'-GACACGGTAGCAGTAGAA-3'

mCCKAR, murine cholecystokinin-A receptor; mCCKBR, murine cholecystokinin-B receptor; mGast, murine gastrin; mHPRT, murine hypoxanthine guanine phosphoribosyl transferase; mCDH1, murine epithelial cadherin or E-cadherin; mTGFB2, murine transforming growth factor- $\beta$  receptor 2.

III In Vivo Optical Imaging System (Perkin Elmer). Mice were distributed at baseline so that tumor flux in each of the four groups was approximately equal.

**Antibody and vaccine treatments.** The anti-gastrin immunogen PAS formerly named Gastrimmune and G17DT (59), is composed of the amino-terminal nine amino acids of G17 gastrin linked to diphtheria toxoid. The G17DT immunogen was renamed PAS, following transfer of ownership to Cancer Advances. PAS comprises a nine amino acid epitope (identical in mouse and humans) derived from the NH<sub>2</sub>-terminal active binding site of gastrin conjugated to diphtheria toxoid in an oil-based adjuvant. PAS is an immunotherapy that stimulated high-affinity polyclonal anti-gastrin antibodies whereas diphtheria toxoid alone had no effect on therapeutic measures (59). Preclinical studies were performed in several animal models with gastrointestinal cancers including colon cancer (40, 47, 50, 53), gastric cancer (46, 58), and pancreatic cancer (41, 44, 49). Antibodies induced by PAS react with a specific epitope on the amino terminus of gastrin and neutralize both amidated and glycine-extended gastrin-17 and do not cross react with CCK or significantly with gastrin-34 (59). PD-1 antibody (Clone RMPI-14) was purchased from Bio X Cell (West Lebanon, NH).

**Study design and treatments.** The overall study design is shown in Fig. 1. At baseline, 1 wk after tumor inoculation (treatment week 0), the mice were divided into 4 groups of 10 mice each with equal tumor size as determined by the IVIS flux luminescent measurement. On day 0, baseline, mice received an intraperitoneal injection in a volume of 100  $\mu$ l of PBS (control), 100  $\mu$ g PAS, 150  $\mu$ g PD-1 antibody (PD-1 Ab), or a combination of PAS and PD-1 Ab. PAS was given three times; at weeks 0, 1, and 3. PD-1 Ab was administered five times on days 0, 4, 8, 15, and 21. Tumor measurements were performed weekly, and volume was calculated based on tumor IVIS flux measured with software from the imaging system described above. When mice became moribund, lost 10% of body weight, or developed ascites, they were ethically euthanized and necropsied. Primary tumors were removed from the pancreas and weighed. All visible metastases were counted, surgically removed, and confirmed by histology.

**TME assessment by histology and immunohistochemistry.** Excised tumors were evaluated histologically with hematoxylin and eosin

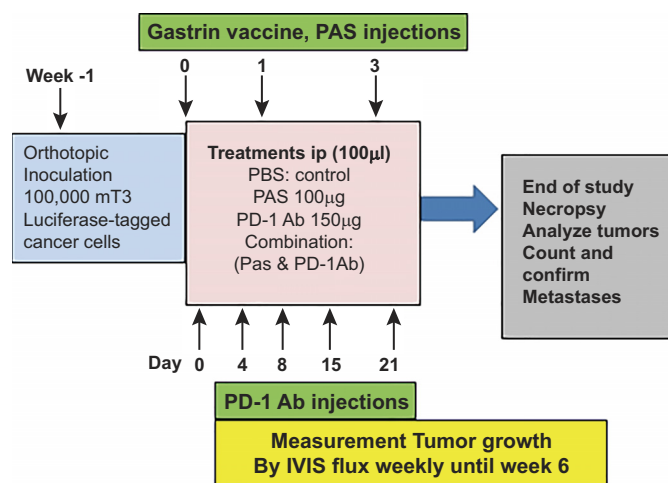


Fig. 1. Study design. Murine pancreatic cancer, mT3, was surgically implanted into the pancreas of C57/BL6 mice at week -1. On day 0 and week 0, therapeutic treatments began. Polyclonal antibody stimulator (PAS) at 100  $\mu$ g was administered by intraperitoneal injection at weeks 0, 1, and 3. Programmed cell death receptor (PD)-1 antibody at 150  $\mu$ g was administered by intraperitoneal injection on days 0, 4, 8, 15, and 21. Tumor growth was monitored weekly by measurement of tumor luciferase activity following luciferin tail-vein injection. Necropsy analysis at the end of the study included measurement of tumor mass and enumeration and localization of metastases.

staining, and intratumoral fibrosis was determined by Masson's trichrome stain. Quantification of fibrosis was performed utilizing computerized software ImageJ by the National Institutes of Health. Metastases were stained with hematoxylin and eosin.

Histological slides (5  $\mu$ m) were prepared from paraffin blocks of tumor tissues. After antigen retrieval was performed with citrate buffer (pH 6), specimens were blocked in 10% normal goat serum at room temperature. Slides were reacted with rabbit polyclonal arginase antibody (cat. no. PA5-29645; ThermoFisher) at a dilution of 1:1,800 to detect M2 macrophages, or with rabbit polyclonal inducible nitric oxide synthase (iNOS) antibody (cat. no. 15323; Abcam) at a dilution of 1:60 to detect M1 macrophages. All slides were reacted with HRP-conjugated anti-rabbit secondary antibody (cat. no. K400311-2; Agilent). Images were taken on an Olympus BX61 microscope with a DP73 camera. The number of immunoreactive cells per slide area was counted with ImageJ computer software by an assistant blinded to the treatments.

**Evaluation of tumor associated genes for EMT.** Total protein from tumor homogenates (20  $\mu$ g) was subjected to gel electrophoresis (NuPAGE 4-12% Bis-Tris Gel; cat. no. NP0321BOX; Invitrogen) and transferred to a nitrocellulose membrane. After being blocked in 5% nonfat milk in Tris-buffered saline, 0.1% Tween 20 (TBST) solution, the blot was incubated overnight at 4°C with primary antibody phospho-paxillin (Tyr118) rabbit polyclonal antibody (1:1,000 dilution; cat. no. 44-722G; ThermoFisher) in 2.5% BSA in PBS, then probed at room temperature for 1 h with a goat anti-rabbit secondary HRP-linked antibody (1:1,000 dilution in 2.5% BSA in TBST solution; ThermoScientific). The nitrocellulose membrane was stripped of antibodies and probed with rabbit polyclonal antibody for total paxillin (1:1,000 dilution in 2.5% BSA TBST solution; cat. no. PA5-79899; ThermoFisher). Protein loading was standardized by measurement of  $\beta$ -actin reactivity following incubation overnight at 4°C with a mouse anti-B-actin antibody (1:5,000 dilution; cat. no. MA1-140; ThermoScientific) followed by incubation for 1 h at room temperature with HRP-conjugated goat anti-mouse secondary antibody (1:1,000 dilution; cat. no. 31430; ThermoScientific). Densitometry was analyzed using a program from ImageJ.

Total protein (20  $\mu$ g) from tumor homogenates was subjected to gel electrophoresis and transferred to nitrocellulose. This blot was probed overnight at 4°C with a primary monoclonal murine antibody to  $\beta$ -catenin (cat. no. 610154, lot: 25190; BD Transduction Laboratories) at a dilution of 1:2,000. This blot was then reacted with HRP-conjugated goat anti-mouse secondary antibody (1:1,000 dilution; cat. no. 31430; ThermoScientific) for 1 h at room temperature. Densitometry was analyzed using a program from ImageJ. Another replicate gel was run with 20  $\mu$ g of protein in each well and transferred to nitrocellulose. This blot was incubated with a primary anti-mouse matrix metalloproteinase-7 (MMP-7; cat. no. 216631; Abcam) antibody overnight at 4°C at a dilution of 1:1,000 and an HRP-conjugated goat anti-mouse secondary antibody (1:1,000 dilution; cat. no. 31430; ThermoScientific) for 1 h at room temperature. Densitometry was analyzed using an area program from ImageJ.

Total RNA was extracted from mT3 tumors with an RNeasy plus Mini Kit (cat. no. 74134; Qiagen, Germantown, MD) to evaluate mRNA expression of *TGF $\beta$ R2* and *E-Cadherin* genes associated with EMT. Complimentary DNA was generated and subjected to real-time PCR (qRT-PCR) using SYBR Green (cat. no. 95073-012; Quanta Biosciences) in an Applied Biosystems 7300 thermal cycler with the following conditions: initial incubation for 3 min at 95°C followed by 40 cycles of 15 s at 95°C and extension 1 min at 60°C using primers with sequence shown in Table 1.

**Statistical analysis.** The weekly growth rate of pancreatic tumors was calculated by comparing the change from baseline in mean bioluminescent flux from all mice in each treatment group over time. Linear regression analysis was performed to compare slopes of the growth curves between each treatment group. The total number of confirmed metastases and the mean number of metastases in each

mouse per treatment group were compared using parametric analysis with ANOVA and Student's *t* test and applying a Bonferroni correction for multiple comparisons to the PBS control mouse group. Mean numbers of immunoreactive cells per area per treatment group ( $n = 10$  each) were compared by ANOVA and Student's *t* test and applying the Bonferroni-correction for multiple comparisons to the PBS control mouse group.

## RESULTS

**Characterization of mT3 murine pancreatic cancer cells.** CCK-B receptor mRNA and gastrin mRNA, but not CCK-A receptor mRNA, were found to be expressed in mT3 cells when total mT3 RNA was subjected to RT-PCR and agarose gel electrophoresis (Fig. 2A). Masson's trichrome stain of an mT3 tumor from an untreated mouse shows dense blue staining consistent with increased fibrosis of the TME (Fig. 2B). The same mT3 tumor from an untreated mouse confirms immunoreactivity with antibody to PD-L1 (Fig. 2C). Confirmation of CCK-B receptor protein expression in mT3 cells was determined by immunofluorescence of antibodies against CCK-B receptor protein and confocal microscopy (Fig. 2D). Gastrin

peptide immunofluorescence was also positive in mT3 cells by confocal microscopy, confirming that these pancreatic cancer cells produce gastrin peptide (Fig. 2E).

**Primary tumor growth and metastases is decreased with PAS vaccine.** Tumor growth as measured weekly by IVIS flux demonstrated that control mice and mice treated with PD-1 antibody had similarly increased tumor growth over time (Fig. 3A). In contrast, orthotopic tumors of mice treated with either PAS100 or PAS100 in combination with PD-1 Ab had relatively decreased tumor growth compared with control over the 6 wk of the study. Tumors in mice treated with PAS100 monotherapy had 81% less flux compared with PBS- and PD-1 Ab-treated mice, but this change did not reach statistical significance ( $P = 0.058$ ). However, tumors of the mice treated with the combination therapy were 97% smaller by flux compared with either PBS- or PD-1 Ab-treated mice (Fig. 3A) and this difference was statistically significant ( $P = 0.0025$ ). These in vivo flux data imply that PAS therapy slowed growth of the primary tumors. Since the mice in this study were not all euthanized on the same day but instead when they became moribund, the final tumor weights were comparable. The final

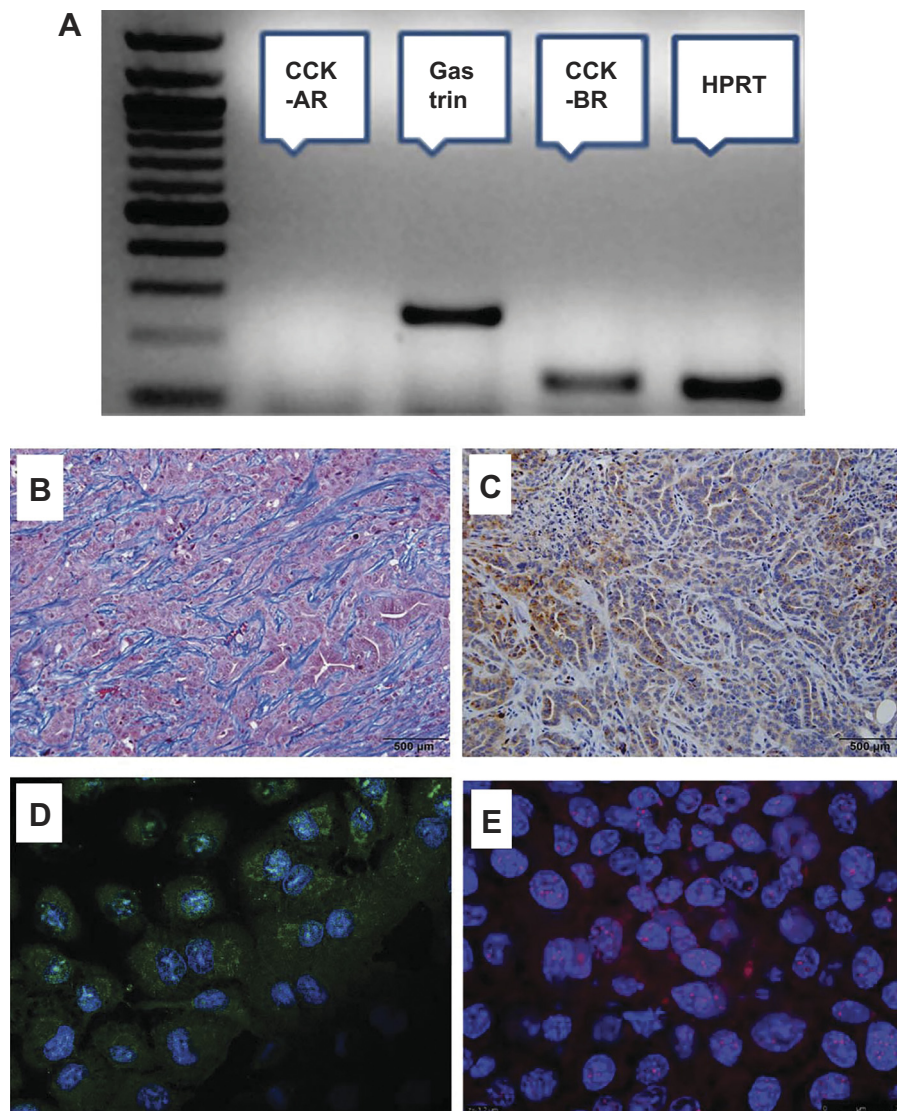


Fig. 2. Characterization of mT3 cells and tumors. A: gel electrophoresis shows DNA ladder and RT-PCR products for the murine cholecystikinin (CCK)-B receptor and gastrin. Hypoxanthine phosphoribosyl transferase (HPRT) serves as a positive control for RNA loading. CCK-A receptor mRNA is not found in the mT3 cells. B: Masson's trichrome stain of an mT3 tumor from an untreated mouse shows extensive intratumoral fibrosis (bar = 500  $\mu$ m). C: immunohistochemistry for the programmed cell death receptor-1 is shown in an mT3 tumor from an untreated mouse (bar = 500  $\mu$ m). D: confocal image of positive immunofluorescence in mT3 cells for the CCK-B receptor. Dylight 488 staining is green and nuclei are stained with Hoechst and are blue. E: confocal image of gastrin immunofluorescence in mT3 cells by confocal microscopy. Gastrin immunoreactivity is stained red with rhodamine, and the nuclei are stained blue with DAPI.

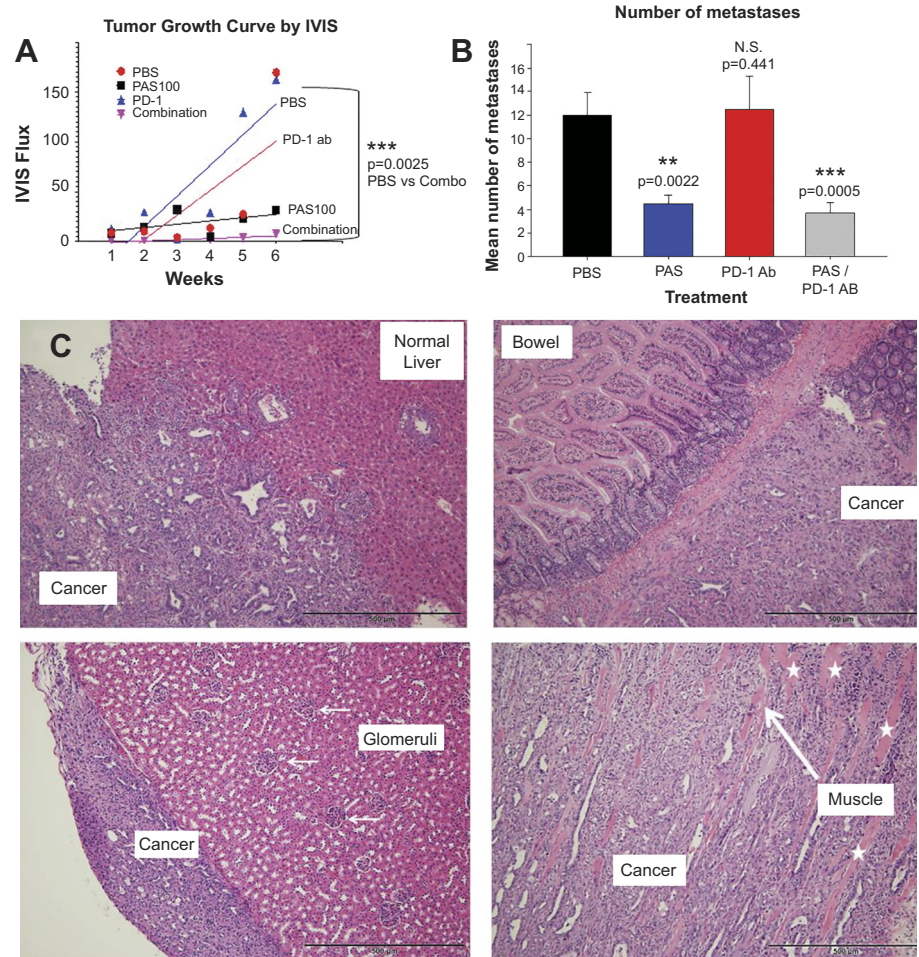


Fig. 3. Tumor growth rate and metastases. *A*: tumor growth rate according to change in IVIS flux. IVIS flux at each week relative to baseline IVIS flux is plotted against number of weeks after beginning of treatment. Tumor growth rates for PBS-treated (circles), polyclonal antibody stimulator (PAS) 100-treated (squares), and programmed cell death receptor (PD)-1 antibody-treated (triangles) mice and mice treated with combination therapy (inverted triangles) are shown. *B*: mean numbers of metastases in PBS-, PAS-, PD-1 Ab-, and PAS/PD-1-Ab-treated mice. *C*: hematoxylin and eosin staining of tissue sections spanning tumor and normal tissue from liver, bowel, kidney, and muscle. \*\*, \*\*\*Significant compared with PBS.

average tumor weight at euthanasia between the groups was similar. For example, the mean tumor weight in the PBS-treated control mice was  $876 \pm 0.225$  mg and the mean tumor weight of the PAS and PD-1 Ab combination group was  $929 \pm 0.193$  mg (not statistically significant). However, despite having similar tumor weights at euthanasia, the average number of metastases in the PAS and PD-1 Ab combination group was significantly lower than in the PBS-treated mice ( $n = 3.7$  compared with  $n = 12$ , respectively). Furthermore, when compared with mice with the same final tumor weight, the PAS-treated mice survived longer. PBS-treated mice survived an average of 50 days, PD-1 Ab mice survived 54 days, PAS monotherapy-treated mice survived 67 days, and mice treated with the combination of PAS and PD-1 Ab survived 70 days. These data suggest that therapy with PAS improves survival and decreases metastases relative to controls.

The mean number of metastases per mouse was significantly reduced in mice treated with PAS monotherapy, or with PAS in combination with PD-1 Ab (Fig. 3*B*). Metastases were abundant in mice treated with either PBS or PD-1 Ab monotherapy. Histologic confirmation of metastases adjacent to or invading normal tissue in liver, bowel, kidney, and muscle is shown in Fig. 3*C*. The specific location and number of metastases in each location according to treatment is shown in Table 2. Most of the metastases occurred in the abdominal cavity and most of them were in the mesentery.

*PAS vaccine and PD-1 antibody therapy decrease fibrosis of the TME.* Intratumoral fibrosis was assessed by staining of collagen fibers in tumor sections with Masson's trichrome stain. Representative histological images from pancreatic tumors of each treatment group consisting of PBS, PD-1 Ab, PAS, and the combination of PAS and PD-1 Ab were reacted

Table 2. Total number and location of metastases in each treatment group

	Liver	Mesentery	Lymph Nodes	Lung	Kidney	Spleen	Rib Cage	Diaphragm	Abdominal Wall	Stomach	Total
PBS	3	39	34	0	8	13	1	10	9	0	117
PAS	5	18	7	0	0	1	0	3	2	0	36
PD-1 Ab	4	55	11	0	6	6	3	9	6	0	100
PAS/PD-1 Ab	0	14	9	1	2	1	0	2	6	2	37

PAS, polyclonal antibody stimulator; PD-1, programmed cell death receptor-1.

with Masson's trichrome stain and are shown in Fig. 4A. Consistent with characteristic features of the pancreatic cancer TME, tumor samples demonstrated marked desmoplastic reaction with increased Masson's trichrome reactivity. Each histologic slide ( $N = 10$  per treatment group) was analyzed by computer software imaging and the mean values (error bars represent standard error of the mean) are shown in graphical form in Fig. 4B. Compared with the PBS control tumors, mean fibrosis scores were significantly increased in mice treated with PD-1 Ab and significantly decreased ( $P = 0.0009$ ) in tumors of mice treated with the combination of PAS and the PD-1 Ab. PAS monotherapy did not significantly change fibrosis of the TME.

*PAS vaccination changes polarization of TAMs.* Consistent with human pancreatic cancer, arginase-positive TAMs with M2 polarization were abundant in tumors of control (PBS-

treated) mice and in mice treated with the PD-1 Ab (Fig. 5A). In contrast, the number of M2 arginase-positive TAMs significantly decreased in tumors of mice treated with PAS monotherapy. Further reduction in M2 TAMs was noted in mice treated with therapy consisting of the combination of PAS with PD-1 Ab. The mean number of immunoreactive M2 TAMs for each group is shown in Fig. 5B. The number of arginase positive TAMs was significantly decreased in tumors of PAS treated mice compared with those of PBS control-treated mice ( $P = 0.017$ ) and in the tumors of PAS and PD-1 combination therapy-treated mice compared with those of the control mice ( $P = 0.0007$  compared with PBS-treated mice, and  $P = 0.02$  compared with PAS monotherapy-treated mice).

In contrast, the number of M1 polarized TAMs in tumors of control PBS-treated mice was detectable, but relatively low,

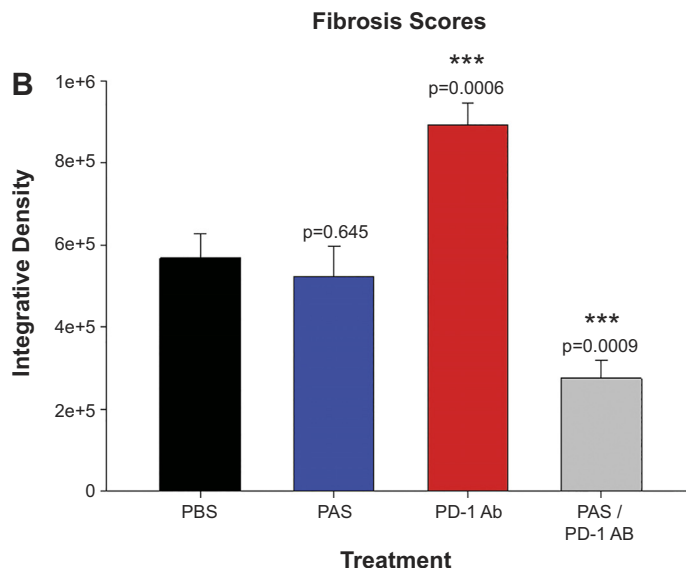
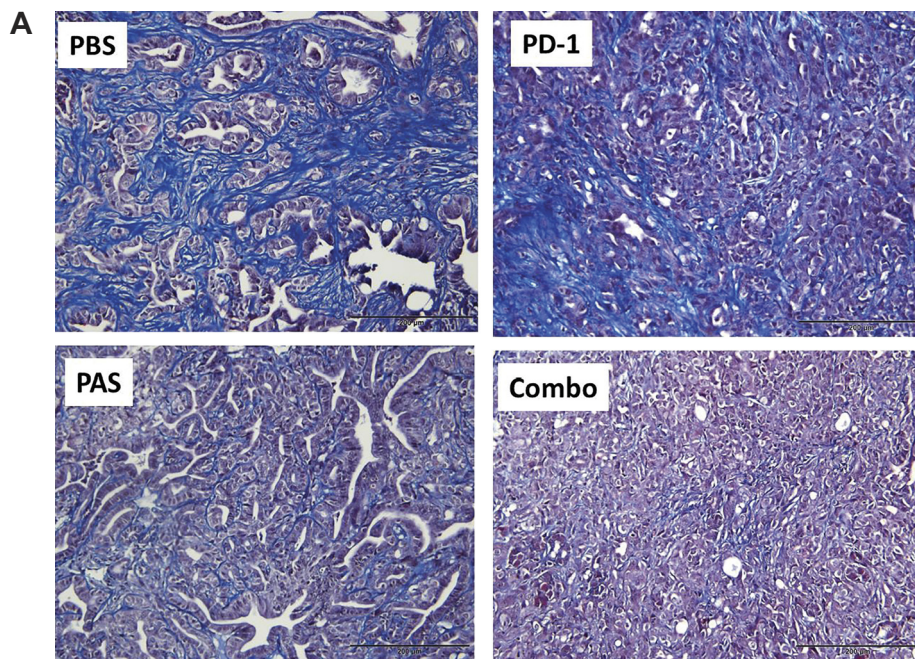


Fig. 4. Tumor-associated fibrosis. A: Masson's trichrome staining of tumor sections from PBS, polyclonal antibody stimulator (PAS), programmed cell death receptor (PD)-1 Ab, and the combination of PAS and PD-1 Ab (Combo). B: quantification of Masson's trichrome staining intensity in tumors from PBS, PAS, PD-1 Ab, and the combination of PAS and PD-1 Ab. \*\*\*Significant compared with PBS.

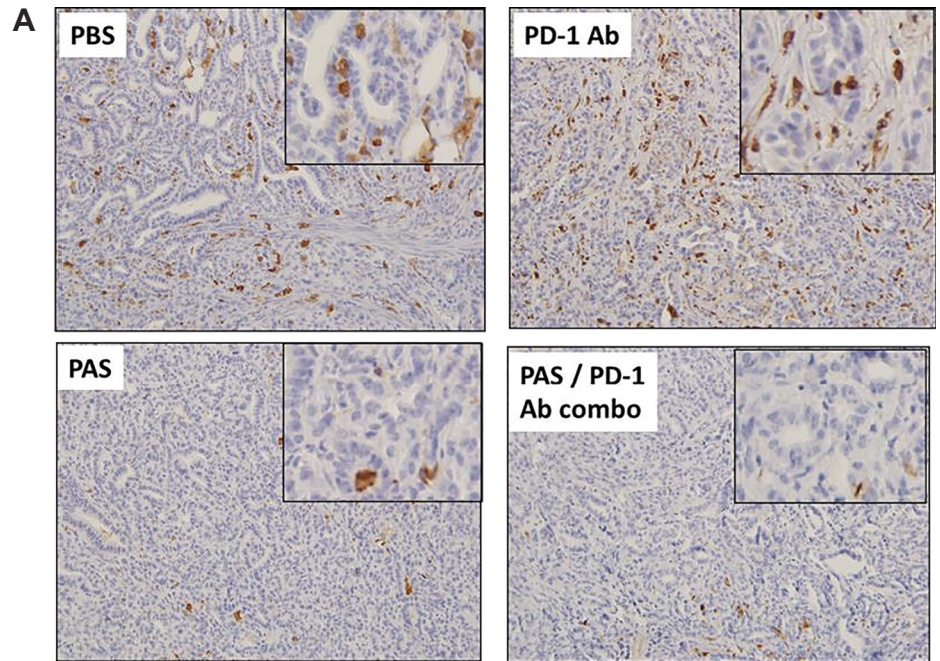
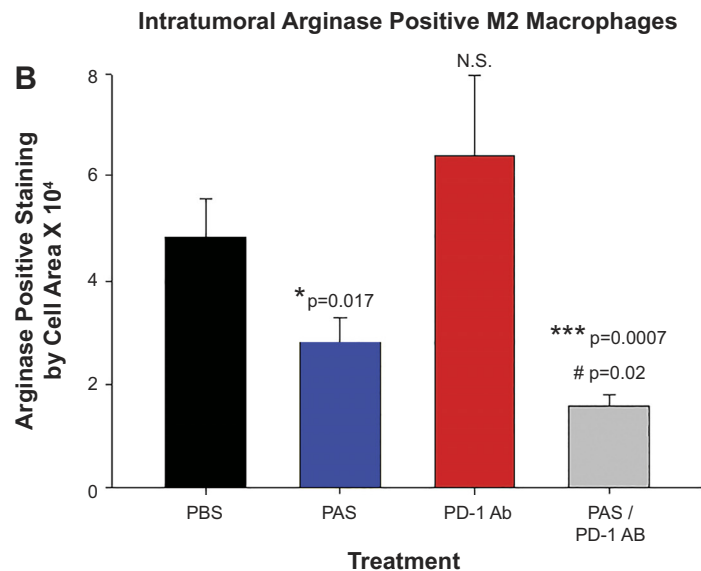


Fig. 5. Tumor-associated macrophages. M2. A: immunostaining of tumor sections for arginase+ phenotypic marker of M2 macrophage phenotype. B: number of arginase-positive cells in tumors of mice treated with PBS, polyclonal antibody stimulator (PAS), programmed cell death receptor (PD)-1 Ab, and PAS/PD-1 Ab combination. \*\*\*, \*Compared with PBS; #compared with PAS.



and this number increased significantly with all treatments (Fig. 6A) as assessed by staining for the M1-specific protein iNOS. Quantification of iNOS-positive cells by computer scanning analysis (Fig. 6B) showed that PAS monotherapy resulted in a nearly 10-fold increase in M1 TAMs relative to control and was statistically significantly higher in tumors from PAS-treated mice than in tumors from PBS-treated mice ( $P = 0.002$ ), and also higher compared with levels in mice receiving the combination therapy.

*PAS decreases metastases by altering EMT-associated genes.* Western blot analysis examination of levels of phosphorylated paxillin in tumors of mice is shown in Fig. 7A. Computer-mediated scanning of density of staining on the Western blot is shown as the ratio of phosphorylated paxillin relative to  $\beta$ -ac-

tin. This analysis determined that the combination of PAS and PD-1 Ab significantly reduced paxillin phosphorylation relative to  $\beta$ -actin ( $P = 0.01$ ) (Fig. 7B).

The epithelial adhesion molecule E-cadherin is also associated with the metastatic potential of tumors, and a decrease in E-cadherin expression is associated with poor outcome in patients with pancreatic cancer (17). Analysis of E-cadherin levels in tumors of mice in this study determined that E-cadherin mRNA levels were 35% higher in tumors of PAS-treated mice compared with PBS-treated mice ( $P = 0.01$ ) (Fig. 7C). Measurement of the TGF $\beta$ 2R was lower in mice vaccinated with PAS compared with PBS controls ( $P = 0.045$ ) (Fig. 7D). These analyses of EMT-associated genes are consistent with both PAS monotherapy, and PAS and PD-1 Ab combi-

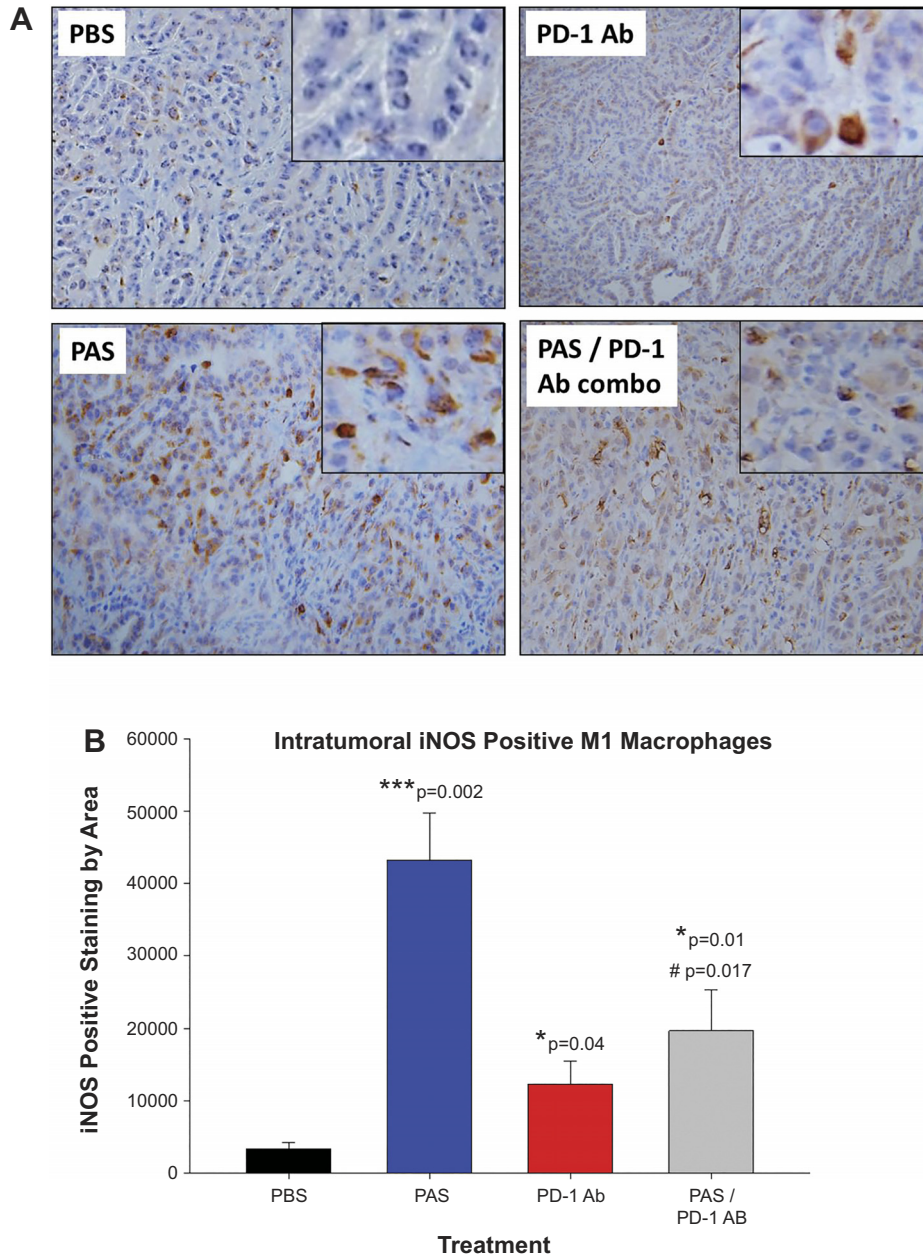


Fig. 6. Tumor-associated macrophages. M1. *A*: immunostaining of tumor sections for inducible nitric oxide synthase (iNOS) phenotypic marker of M1 macrophage phenotype. *B*: number of iNOS-positive cells in tumors of mice treated with PBS, polyclonal antibody stimulator (PAS), programmed cell death receptor (PD)-1 Ab, and PAS/PD-1 Ab combination. \*\*\*, \*Compared with PBS; #compared with PAS.

nation therapy having specific effects on the ability of pancreatic tumors to metastasize.

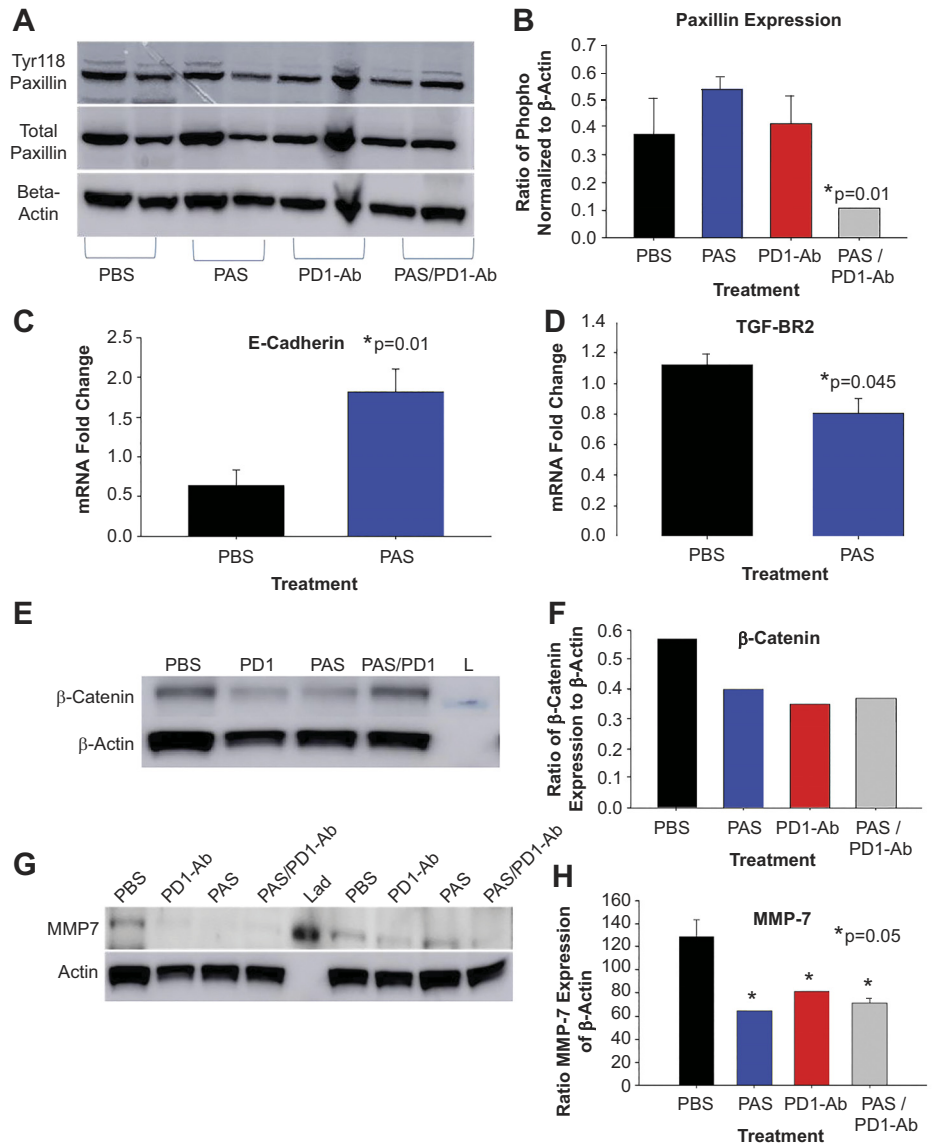
Western blot of total tumor protein demonstrated less  $\beta$ -catenin (Fig. 7, *E* and *F*) in tumors of PAS-treated mice and significantly less MMP-7 (Fig. 7, *G* and *H*) in tumors of mice receiving the combination PAS and PD-1 Ab.

## DISCUSSION

The present investigation demonstrates that a vaccination directed against gastrin decreases pancreatic tumor growth and metastases and improves survival. Treatment with PD-1 antibody monotherapy had no effect on growth of pancreatic cancer; however, when PD-1 Ab was given in combination with PAS, changes in the TME were observed. Among these changes was a decrease in dense desmoplastic fibrosis in the TME that has been shown to impede the penetration of che-

motherapeutic agents and immunotherapy. Vaccination with PAS also significantly altered the balance of the tumor-associated macrophage population in mouse tumors. Macrophages with M2-like phenotype are known to be protumorigenic. This population was abundant in tumors of PBS-treated mice but was significantly decreased in tumors of mice vaccinated with PAS. In contrast, the proinflammatory or M1 macrophage population was increased in tumors of PAS-treated mice. This polarization change from M2 to M1 macrophages may have contributed to the decreased primary tumor size and remodeling of the TME with less fibrosis. Macrophages have trophic properties (35) especially by promoting angiogenesis. The recruitment and accumulation of TAMs are regulated by chemokine ligands released by tumor and stromal cells (2). CxCR4 is a major chemokine involved in this process (18). The expression of CxCR4 is regulated by TGF- $\beta$  (3). We

Fig. 7. Molecular markers and proteins associated with metastases. **A:** Western blot of total protein from tumor samples from mice treated with PBS, polyclonal antibody stimulator (PAS), programmed cell death receptor (PD)-1 Ab, and PAS/PD-1 Ab combination probed with antibody specific for Tyr118 phosphorylated paxillin (*top*), total paxillin (*middle*), and  $\beta$ -actin (*bottom*). **B:** ratio of phosphorylated paxillin relative to  $\beta$ -actin plotted for each treatment group (\* $P = 0.01$ , compared with PBS). **C:** change in E-cadherin mRNA in tumors of PAS-treated mice relative to PBS control. **D:** change in tumor necrosis factor- $\beta$  receptor 2 (TGF- $\beta$ R2) mRNA in tumors of PAS-treated mice relative to PBS control. **E:** Western blot of total protein from tumor samples probed with  $\beta$ -catenin and  $\beta$ -actin. L, ladder. **F:** levels of  $\beta$ -catenin protein relative to  $\beta$ -actin in tumors of treated mice. **G:** Western blot of total protein from tumor samples probed with mouse matrix metalloproteinase-7 (MMP-7) and  $\beta$ -actin. Lad, ladder. **H:** levels of MMP-7 protein relative to  $\beta$ -actin in tumor samples (see Graphical Abstract). Effect of PAS on epithelial-mesenchymal transition (EMT) and tumor metastases. Gastrin stimulates growth and metastasis of pancreatic cancer through activation of the cholecystokinin (CCK-BR) receptor. In tumors of PBS-treated mice, the tumor microenvironment has extensive fibrosis and M2 tumor associated macrophages. The macrophages release CxCR4 to activate TGF- $\beta$  signaling. The cancer epithelial cells undergo EMT through a metastatic cascade process that involves disruption in the adherens junctions associated with loss of E-cadherin. Gastrin activates phosphorylation of the focal adhesion protein paxillin and activation of the MMP-7 promoter increasing  $\beta$ -catenin expression and nuclear translocation leading to cell migration. Vaccination with PAS interrupts the action of gastrin leading to decreased fibrosis of the tumor microenvironment and reversing EMT, thus decreasing metastases. \*Significant compared with PBS.



previously demonstrated that CxCR4 expression is significantly decreased in tumors of mice treated with a nanoparticle and a siRNA to decrease gastrin expression. Current investigations are exploring the targeting of chemokines to decrease recruitment of immunosuppressive TAMs (2). PD-1 receptors have been extensively studied in T-lymphocytes but less studied in TAMs. Recent studies demonstrate that the M2 macrophages express more PD-1 than the M1 TAMs (16). One possible mechanism for our findings could be that PAS changes the PD-1 expression on TAMs, thus making the combination therapy with PAS and the PD-1 Ab more effective.

Tumor fibrosis was significantly reduced in mice that received the combination of PAS and PD-1 Ab. The dense stroma of the pancreatic TME has been shown to impede penetration of chemotherapeutic agents and immune cells (19). The fibroblast is responsible for the dense stroma and other important components of the TME (1, 56). Because our study was performed with orthotopic tumors in the mouse pancreas, many of these fibroblasts were most likely derived from acti-

vated pancreatic stellate cells. In pancreatic cancer, additional recruitment of myofibroblasts are derived from mesenchymal precursors in the circulation (61). Cancer-associated fibroblasts (CAFs) secrete proteins in the ECM as well as soluble factors that stimulate cancer progression. These CAFs are thought to be derived from mesenchymal cells from different origins that are either resident or recruited to the pancreas by neoplastic cells (32). Two distinct populations of CAFs have been identified: 1) inflammatory fibroblasts and 2) myofibroblasts (32). Elimination of Sonic Hedge Hog signaling eliminates the myofibroblasts and  $\alpha$ -smooth muscle actin of the microenvironment, thus rendering pancreatic cancer more aggressive and metastatic (37). In contrast, strategies that decrease the inflammatory fibroblasts and fibroblast-activated protein are associated with decreased cancer growth and metastases (14, 21). In a recent study, mice bearing orthotopic gastrin-producing mT5 murine pancreatic tumors, and treated with a CCK-B receptor antagonist proglumide, had fewer metastases (30). In addition, tumors of these mice had similar  $\alpha$ -smooth muscle actin immunoreactivity compared with tumors of PBS controls.

Since fewer metastases were also observed in the PAS-treated mice in this investigation, most likely the fibroblast-activated protein-producing inflammatory fibroblasts were decreased with PAS.

In this study, we demonstrated that PAS vaccination is effective in reducing metastases by decreasing the key pathway proteins involved in EMT (see Graphical Abstract). This characteristic feature of decreasing metastases is unique to PAS monotherapy alone and independent of PD-1 Ab treatment. Watson and colleagues (60) previously showed that passive immunization with rabbit PAS-induced antibodies decreased the number and size of metastases of colorectal cancer in an immune deficient mouse. We formerly demonstrated that a nanoparticle delivering siRNA to gastrin also completely prevented metastases in athymic nude mice bearing human pancreatic tumors (8). Thus strategies that decrease circulating or endogenous tumor production of gastrin have been shown to inhibit metastases from gastrointestinal cancers. Specific components of the metastasis cascade and EMT, including protein expression of paxillin,  $\beta$ -catenin, and MMP-7, were effectively diminished with the combination of PAS and the PD-1 Ab therapy. Site-specific phosphorylation of paxillin has been shown to be correlated with gastrin-dependent migration of pancreatic cancer cells in vitro (29). Mu and colleagues (29) have demonstrated that gastrin promotes the reorientation of the Golgi apparatus and directional migration of pancreatic cancer cells by inducing the activation of paxillin and FAK via the CCK-B receptor  $G\alpha_{12/13}$ -RhoA-ROCK signaling pathway. Cell migration requires reorientation of the cell secretory machinery; this process is accomplished in coordination with a rearrangement of the cytoskeleton and focal adhesion formation (63). We demonstrated that when gastrin is decreased through vaccination with PAS, less phosphorylation of paxillin at Tyr118 occurs, resulting in decreased recruitment of FAK and Src kinases. In cancer, gastrin signals through the noncanonical pathway by activation of cellular Src and transactivation of receptor tyrosine kinases (27, 42); however, in the absence of gastrin using genetically engineered gastrin-knockout/*Kras* mice, the transactivation mitogenic pathway through Src kinase phosphorylation is significantly reduced (31).

The metalloproteinase MMP-7 expression has been shown to be upregulated by gastrin in a gastric cancer model with *Helicobacter pylori* and decreased gastrin expression via RNAi methodology reduced MMP-7 protein expression (12, 66). Gastrin activates the MMP-7 promoter by involvement of serine/threonine kinase glycogen synthase kinase-3  $\beta$  (GSK3 $\beta$ ) (26). Snail and  $\beta$ -catenin are both downstream targets of GSK3 $\beta$  (69). Gastrin activates two independent signaling axes both of which lead to MMP-7 transcription and cell migration: the first one involves activation of MLK3/JNK1 axis (26), and the second involves inhibition of GSK3 $\beta$  axis leading to an induction of Snail expression and  $\beta$ -catenin nuclear translocation. Vaccination of mice with PAS in combination with the PD-1 Ab resulted in decreased MMP-7 and  $\beta$ -catenin expression in mT3 tumors in this current study, supporting the mechanism through which gastrin neutralization can decrease migration, EMT and subsequent metastases.

Several proteinases are known to cleave E-cadherin, including MMP-7. MMP-7-mediated E-cadherin cleavage induces cell migration with loss of contact inhibition and an increase in proliferation (23), and E-cadherin also modulates important

signaling molecules such as  $\beta$ -catenin. Gastrin has been shown to increase metastases by inducing  $\beta$ -catenin nuclear translocation (70). Vaccination with PAS reduces gastrin resulting in a decrease in  $\beta$ -catenin expression.

TGF- $\beta$ 1 combines with TGF $\beta$ 2 to activate TGF- $\beta$  signaling, an important pathway involved in proliferation, apoptosis, EMT, and metastasis in various cancers. Neutralization of TGF $\beta$ 2 in murine pancreatic cancer has been shown to inhibit metastases (33). TGF- $\beta$  signaling also induces immune suppression within the TME resulting in tumor immune evasion and poor responses to cancer immunotherapy (4). Therefore, suppressing activation of the TGF- $\beta$  signaling pathway with PAS vaccination may have improved efficacy of the PD-1 Ab.

This investigation confirmed that therapy with PAS, a vaccination that induces neutralizing antibodies to gastrin and activates T-cell immunity, inhibits pancreatic cancer metastases by interruption of EMT. PAS also collaborates with PD-1 Ab to decrease fibrosis of the TME rendering the tumor susceptible to the penetration of immunotherapy and perhaps chemotherapy. Tumor immune cell signature and TAMs, in particular, are phenotypically modified to become more proinflammatory and less immunosuppressive by administration of PAS. In conclusion, gastrin is an important driver of pancreatic cancer growth and metastases; therefore, strategies to interrupt or neutralize the actions of gastrin signaling at the CCK-B receptor may improve survival of patients with pancreatic cancer.

#### ACKNOWLEDGMENTS

We appreciate the technical support from the staff in the Lombardi Core Histology laboratory. We also appreciate the staff in the animal care facility.

#### GRANTS

This study was funded in part by a grant from Cancer Advances, Inc. and its subsidiary Vaccicure, Ltd., National Center for Advancing Translational Sciences Training Grant TL1-TR-001431 (for S. Nadella), and National Cancer Institute Grant CA-051008 (to the Georgetown Lombardi Cancer Center Core facilities).

#### DISCLOSURES

Cato Research (Durham, NC) has intellectual property rights for polyclonal antibody stimulator (PAS). PAS compound was transferred to Georgetown University by a Material Transfer agreement with Vaccicure, Ltd., Liverpool, UK for this research project. All authors work for Cato Research or Georgetown University.

#### AUTHOR CONTRIBUTIONS

J.P.S., N.O., R.S., L.S. and A.C. conceived and designed research; J.P.S., M.D.G., H.C., R.D.T., and X.L. performed experiments; J.P.S., N.O., R.S., S.N., S.W., M.D.G., H.C., L.S., and A.C. analyzed data; J.P.S., N.O., R.S., M.D.G., H.C., A.K., L.S., and A.C. interpreted results of experiments; J.P.S., M.D.G., S.N. S.W. and H.C. prepared figures; J.P.S., S.W., and S.N. drafted manuscript; N.O., R.S., M.D.G., H.C., R.D.T., X.L., A.K., L.S., A.C. AND J.P.S. edited and revised manuscript; ALL authors approved final version of manuscript.

#### REFERENCES

1. Apte MV, Wilson JS, Lugea A, Pandolfi SJ. A starring role for stellate cells in the pancreatic cancer microenvironment. *Gastroenterology* 144: 1210–1219, 2013. doi:10.1053/j.gastro.2012.11.037.
2. Argyle D, Kitamura T. Targeting macrophage-recruiting chemokines as a novel therapeutic strategy to prevent the progression of solid tumors. *Front Immunol* 9: 2629, 2018. doi:10.3389/fimmu.2018.02629.
3. Arwert EN, Harney AS, Entenberg D, Wang Y, Sahai E, Pollard JW, Condeelis JS. A Unidirectional transition from migratory to perivascular

- macrophage is required for tumor cell intravasation. *Cell Rep* 23: 1239–1248, 2018. doi:10.1016/j.celrep.2018.04.007.
4. **Battle E, Massagué J.** Transforming growth factor- $\beta$  signaling in immunity and cancer. *Immunity* 50: 924–940, 2019. doi:10.1016/j.immuni.2019.03.024.
  5. **Bierie B, Moses HL.** Transforming growth factor beta (TGF- $\beta$ ) and inflammation in cancer. *Cytokine Growth Factor Rev* 21: 49–59, 2010. doi:10.1016/j.cytogfr.2009.11.008.
  6. **Biswas SK, Mantovani A.** Macrophage plasticity and interaction with lymphocyte subsets: cancer as a paradigm. *Nat Immunol* 11: 889–896, 2010. doi:10.1038/ni.1937.
  7. **Boj SF, Hwang CI, Baker LA, Chio II, Engle DD, Corbo V, Jager M, Ponz-Sarvise M, Tiriach H, Spector MS, Gracanin A, Oni T, Yu KH, van Boxtel R, Huch M, Rivera KD, Wilson JP, Feigin ME, Öhlund D, Handly-Santana A, Ardito-Abraham CM, Ludwig M, Elyada E, Alagesan B, Biffi G, Yordanov GN, Delcuze B, Creighton B, Wright K, Park Y, Morsink FHM, Molenaar IQ, Borel Rinkes IH, Cuppen E, Hao Y, Jin Y, Nijman IJ, Iacobuzio-Donahue C, Leach SD, Pappin DJ, Hammell M, Klimstra DS, Basturk O, Hruban RH, Offerhaus GJ, Vries RGJ, Clevers H, Tuveson DA, van BR, Morsink FH, Molenaar IQ, Borel Rinkes IH, Cuppen E, Hao Y, Jin Y, Nijman IJ, Iacobuzio-Donahue C, Leach SD, Pappin DJ, Hammell M, Klimstra DS, Basturk O, Hruban RH, Offerhaus GJ, Vries RG, Clevers H, Tuveson DA.** Organoid models of human and mouse ductal pancreatic cancer. *Cell* 160: 324–338, 2015. doi:10.1016/j.cell.2014.12.021.
  8. **Burks J, Nadella S, Mahmud A, Mankongpaisarnrung C, Wang J, Hahn JJ, Tucker RD, Shivapurkar N, Stern ST, Smith JP.** Cholecystokinin receptor-targeted polyplex nanoparticle inhibits growth and metastasis of pancreatic cancer. *Cell Mol Gastroenterol Hepatol* 6: 17–32, 2018. doi:10.1016/j.jcmgh.2018.02.013.
  9. **Cao H, Le D, Yang LX.** Current status in chemotherapy for advanced pancreatic adenocarcinoma. *Anticancer Res* 33: 1785–1791, 2013.
  10. **Condeelis J, Pollard JW.** Macrophages: obligate partners for tumor cell migration, invasion, and metastasis. *Cell* 124: 263–266, 2006. doi:10.1016/j.cell.2006.01.007.
  12. **Dickson JH, Grabowska A, El-Zaatari M, Atherton J, Watson SA.** *Helicobacter pylori* can induce heparin-binding epidermal growth factor expression via gastrin and its receptor. *Cancer Res* 66: 7524–7531, 2006. doi:10.1158/0008-5472.CAN-05-3246.
  13. **Ellrichmann M, Ritter PR, Schrader H, Schmidt WE, Meier JJ, Schmitz F.** Gastrin stimulates the VEGF-A promoter in a human colon cancer cell line. *Regul Pept* 165: 146–150, 2010. doi:10.1016/j.regpep.2010.06.004.
  14. **Fan MH, Zhu Q, Li HH, Ra HJ, Majumdar S, Gulick DL, Jerome JA, Madsen DH, Christofidou-Solomidou M, Speicher DW, Bachovchin WW, Feghali-Bostwick C, Puré E.** Fibroblast activation protein (FAP) accelerates collagen degradation and clearance from lungs in mice. *J Biol Chem* 291: 8070–8089, 2016. doi:10.1074/jbc.M115.701433.
  15. **Gilliam AD, Broome P, Topuzov EG, Garin AM, Pelay I, Humphreys J, Whitehead A, Takhar A, Rowlands BJ, Beckingham IJ.** An international multicenter randomized controlled trial of G17DT in patients with pancreatic cancer. *Pancreas* 41: 374–379, 2012. doi:10.1097/MPA.0b013e31822ade7e.
  16. **Gordon SR, Maute RL, Dulken BW, Hutter G, George BM, McCracken MN, Gupta R, Tsai JM, Sinha R, Corey D, Ring AM, Connolly AJ, Weissman IL.** PD-1 expression by tumour-associated macrophages inhibits phagocytosis and tumour immunity. *Nature* 545: 495–499, 2017. doi:10.1038/nature22396.
  17. **Hong SM, Li A, Olino K, Wolfgang CL, Herman JM, Schulick RD, Iacobuzio-Donahue C, Hruban RH, Goggins M.** Loss of E-cadherin expression and outcome among patients with resectable pancreatic adenocarcinomas. *Mod Pathol* 24: 1237–1247, 2011. doi:10.1038/modpathol.2011.74.
  18. **Hughes R, Qian BZ, Rowan C, Muthana M, Keklikoglou I, Olson OC, Tazzyman S, Danson S, Addison C, Clemons M, Gonzalez-Angulo AM, Joyce JA, De Palma M, Pollard JW, Lewis CE.** Perivascular M2 macrophages stimulate tumor relapse after chemotherapy. *Cancer Res* 75: 3479–3491, 2015. doi:10.1158/0008-5472.CAN-14-3587.
  19. **Hwang RF, Moore T, Arumugam T, Ramachandran V, Amos KD, Rivera A, Ji B, Evans DB, Logsdon CD.** Cancer-associated stromal fibroblasts promote pancreatic tumor progression. *Cancer Res* 68: 918–926, 2008. doi:10.1158/0008-5472.CAN-07-5714.
  20. **Kalluri R, Weinberg RA.** The basics of epithelial-mesenchymal transition. *J Clin Invest* 119: 1420–1428, 2009. doi:10.1172/JCI39104.
  21. **Kraman MO, Bambrough PJ, Arnold JN, Roberts EW, Magiera L, Jones JM, Gopinathan A, Tuveson DA, Fearon DT.** Suppression of antitumor immunity by stromal cells expressing fibroblast activation protein- $\alpha$ . *Science* 330: 827–830, 2010. doi:10.1126/science.1195300.
  22. **López-Colomé AM, Lee-Rivera I, Benavides-Hidalgo R, López E.** Paxillin: a crossroad in pathological cell migration. *J Hematol Oncol* 10: 50, 2017. doi:10.1186/s13045-017-0418-y.
  23. **Lynch CC, Vargo-Gogola T, Matrisian LM, Fingleton B.** Cleavage of E-Cadherin by matrix metalloproteinase-7 promotes cellular proliferation in nontransformed cell lines via activation of RhoA. *J Oncol* 2010: 530745, 2010. doi:10.1155/2010/530745.
  24. **Martin T, Ye L, Sanders AJ, Lane J, Jiang WG.** Cancer invasion and metastasis: molecular and cellular perspective. In: *Madame Curie Bioscience Database*, edited by Jandial R. Austin, TX: Landes Bioscience, 2013.
  25. **Mendonsa AM, Na TY, Gumbiner BM.** E-cadherin in contact inhibition and cancer. *Oncogene* 37: 4769–4780, 2018. doi:10.1038/s41388-018-0304-2.
  26. **Mishra P, Senthivayagam S, Rana A, Rana B.** Glycogen synthase kinase-3 $\beta$  regulates Snail and beta-catenin during gastrin-induced migration of gastric cancer cells. *J Mol Signal* 5: 9, 2010. doi:10.1186/1750-2187-5-9.
  27. **Moody TW, Nuche-Berenguer B, Moreno P, Jensen RT.** CI-988 Inhibits EGFR transactivation and proliferation caused by addition of CCK/gastrin to lung cancer cells. *J Mol Neurosci* 56: 663–672, 2015. doi:10.1007/s12031-015-0533-6.
  29. **Mu G, Ding Q, Li H, Zhang L, Zhang L, He K, Wu L, Deng Y, Yang D, Wu L, Xu M, Zhou J, Yu H.** Gastrin stimulates pancreatic cancer cell directional migration by activating the G $\alpha$ 12/13-RhoA-ROCK signaling pathway. *Exp Mol Med* 50: 59, 2018. doi:10.1038/s12276-018-0081-6.
  30. **Nadella S, Burks J, Al-Sabban A, Inyang G, Wang J, Tucker RD, Zamanis ME, Bukowski W, Shivapurkar N, Smith JP.** Dietary fat stimulates pancreatic cancer growth and promotes fibrosis of the tumor microenvironment through the cholecystokinin receptor. *Am J Physiol Gastrointest Liver Physiol* 315: G699–G712, 2018. doi:10.1152/ajpgi.00123.2018.
  31. **Nadella S, Burks J, Huber M, Wang J, Cao H, Kallakury B, Tucker RD, Boca SM, Jermusyck A, Collins I, Vietsch EE, Pierobon M, Hodge KA, Cui W, Amundadottir LT, Petricoin E 3rd, Shivapurkar N, Smith JP.** Endogenous gastrin collaborates with mutant KRAS in pancreatic carcinogenesis. *Pancreas* 48: 894–903, 2019. doi:10.1097/MPA.0000000000001360.
  32. **Öhlund D, Handly-Santana A, Biffi G, Elyada E, Almeida AS, Ponz-Sarvise M, Corbo V, Oni TE, Hearn SA, Lee EJ, Chio II, Hwang CI, Tiriach H, Baker LA, Engle DD, Feig C, Kultti A, Egeblad M, Fearon DT, Crawford JM, Clevers H, Park Y, Tuveson DA.** Distinct populations of inflammatory fibroblasts and myofibroblasts in pancreatic cancer. *J Exp Med* 214: 579–596, 2017.
  33. **Ostapoff KT, Cenik BK, Wang M, Ye R, Xu X, Nugent D, Hagopian MM, Topalovski M, Rivera LB, Carroll KD, Brekken RA.** Neutralizing murine TGF $\beta$ R2 promotes a differentiated tumor cell phenotype and inhibits pancreatic cancer metastasis. *Cancer Res* 74: 4996–5007, 2014. doi:10.1158/0008-5472.CAN-13-1807.
  34. **Pedone E, Marucci L.** Role of  $\beta$ -catenin activation levels and fluctuations in controlling cell fate. *Genes (Basel)* 10: 176, 2019. doi:10.3390/genes10020176.
  35. **Pollard JW.** Trophic macrophages in development and disease. *Nat Rev Immunol* 9: 259–270, 2009. doi:10.1038/nri2528.
  36. **Qian BZ, Pollard JW.** Macrophage diversity enhances tumor progression and metastasis. *Cell* 141: 39–51, 2010. doi:10.1016/j.cell.2010.03.014.
  37. **Rhim AD, Oberstein PE, Thomas DH, Mirek ET, Palermo CF, Sastra SA, Dekleva EN, Saunders T, Becerra CP, Tattersall IW, Westphalen CB, Kitajewski J, Fernandez-Barrera MG, Fernandez-Zapico ME, Iacobuzio-Donahue C, Olive KP, Stanger BZ.** Stromal elements act to restrain, rather than support, pancreatic ductal adenocarcinoma. *Cancer Cell* 25: 735–747, 2014. doi:10.1016/j.ccr.2014.04.021.
  38. **Sica A, Larghi P, Mancino A, Rubino L, Porta C, Totaro MG, Rimoldi M, Biswas SK, Allavena P, Mantovani A.** Macrophage polarization in tumour progression. *Semin Cancer Biol* 18: 349–355, 2008. doi:10.1016/j.semcancer.2008.03.004.
  39. **Sideras K, Braat H, Kwekkeboom J, van Eijck CH, Peppelenbosch MP, Sleijfer S, Bruno M.** Role of the immune system in pancreatic cancer progression and immune modulating treatment strategies. *Cancer Treat Rev* 40: 513–522, 2014. [Erratum in *Cancer Treat Rev* 40: 892, 2014.] doi:10.1016/j.ctrv.2013.11.005.

40. **Singh P, Walker JP, Townsend CM Jr, Thompson JC.** Role of gastrin and gastrin receptors on the growth of a transplantable mouse colon carcinoma (MC-26) in BALB/c mice. *Cancer Res* 46: 1612–1616, 1986.
41. **Smith JP, Fantasley AP, Liu G, Zagon IS.** Identification of gastrin as a growth peptide in human pancreatic cancer. *Am J Physiol Regul Integr Comp Physiol* 268: R135–R141, 1995. doi:10.1152/ajpregu.1995.268.1.R135.
42. **Smith JP, Fonkousa LK, Moody TW.** The Role of gastrin and CCK receptors in pancreatic cancer and other malignancies. *Int J Biol Sci* 12: 283–291, 2016. doi:10.7150/ijbs.14952.
43. **Smith JP, Hamory MW, Verderame MF, Zagon IS.** Quantitative analysis of gastrin mRNA and peptide in normal and cancerous human pancreas. *Int J Mol Med* 2: 309–315, 1998. doi:10.3892/ijmm.2.3.309.
44. **Smith JP, Kramer ST, Solomon TE.** CCK stimulates growth of six human pancreatic cancer cell lines in serum-free medium. *Regul Pept* 32: 341–349, 1991. doi:10.1016/0167-0115(91)90027-E.
45. **Smith JP, Shih A, Wu Y, McLaughlin PJ, Zagon IS.** Gastrin regulates growth of human pancreatic cancer in a tonic and autocrine fashion. *Am J Physiol Regul Integr Comp Physiol* 270: R1078–R1084, 1996. doi:10.1152/ajpregu.1996.270.5.R1078.
46. **Smith JP, Shih AH, Wotring MG, McLaughlin PJ, Zagon IS.** Characterization of CCK-B/gastrin-like receptors in human gastric carcinoma. *Int J Oncol* 12: 411–419, 1998. doi:10.3892/ijo.12.2.411.
47. **Smith JP, Solomon TE.** Effects of gastrin, proglumide, and somatostatin on growth of human colon cancer. *Gastroenterology* 95: 1541–1548, 1988. doi:10.1016/S0016-5085(88)80075-1.
48. **Smith JP, Solomon TE.** Cholecystokinin and pancreatic cancer: the chicken or the egg? *Am J Physiol Gastrointest Liver Physiol* 306: G91–G101, 2014. doi:10.1152/ajpgi.00301.2013.
49. **Smith JP, Solomon TE, Bagheri S, Kramer S.** Cholecystokinin stimulates growth of human pancreatic adenocarcinoma SW-1990. *Dig Dis Sci* 35: 1377–1384, 1990. doi:10.1007/BF01536744.
50. **Smith JP, Stock EA, Wotring MG, McLaughlin PJ, Zagon IS.** Characterization of the CCK-B/gastrin-like receptor in human colon cancer. *Am J Physiol Regul Integr Comp Physiol* 271: R797–R805, 1996. doi:10.1152/ajpregu.1996.271.3.R797.
51. **Smith JP, Wang S, Nadella S, Jablonski SA, Weiner LM.** Cholecystokinin receptor antagonist alters pancreatic cancer microenvironment and increases efficacy of immune checkpoint antibody therapy in mice. *Cancer Immunol Immunother* 67: 195–207, 2018. doi:10.1007/s00262-017-2077-9.
52. **Sousa B, Pereira J, Paredes J.** The crosstalk between cell adhesion and cancer metabolism. *Int J Mol Sci* 20: 1933, 2019. doi:10.3390/ijms20081933.
53. **Upp JR Jr, Singh P, Townsend CM Jr, Thompson JC.** Clinical significance of gastrin receptors in human colon cancers. *Cancer Res* 49: 488–492, 1989.
54. **van Roy F, Berx G; van RF and Berx G.** The cell-cell adhesion molecule E-cadherin. *Cell Mol Life Sci* 65: 3756–3788, 2008. doi:10.1007/s00018-008-8281-1.
55. **Vonderheide RH, Bayne LJ.** Inflammatory networks and immune surveillance of pancreatic carcinoma. *Curr Opin Immunol* 25: 200–205, 2013. doi:10.1016/j.coi.2013.01.006.
56. **Waghray M, Yalamanchili M, di Magliano MP, Simeone DM.** Deciphering the role of stroma in pancreatic cancer. *Curr Opin Gastroenterol* 29: 537–543, 2013. doi:10.1097/MOG.0b013e328363affe.
57. **Wang S, Huang S, Sun YL.** Epithelial-mesenchymal transition in pancreatic cancer: A review. *Biomed Res Int* 2017: 2646148, 2017. doi:10.1155/2017/2646148.
58. **Watson S, Durrant L, Morris D.** Gastrin: growth enhancing effects on human gastric and colonic tumour cells. *Br J Cancer* 59: 554–558, 1989. doi:10.1038/bjc.1989.112.
59. **Watson SA, Michaeli D, Grimes S, Morris TM, Robinson G, Varro A, Justin TA, Hardcastle JD.** Gastrin raises antibodies that neutralize amidated and glycine-extended gastrin-17 and inhibit the growth of colon cancer. *Cancer Res* 56: 880–885, 1996.
60. **Watson SA, Michaeli D, Morris TM, Clarke P, Varro A, Griffin N, Smith A, Justin T, Hardcastle JD.** Antibodies raised by gastrin immunize inhibit the spontaneous metastasis of a human colorectal tumour, AP5LV. *Eur J Cancer* 35: 1286–1291, 1999. doi:10.1016/S0959-8049(99)00115-X.
61. **Whittle MC, Hingorani SR.** Fibroblasts in pancreatic ductal adenocarcinoma: biological mechanisms and therapeutic targets. *Gastroenterology* 156: 2085–2096, 2019. doi:10.1053/j.gastro.2018.12.044.
62. **Wyckoff J, Wang W, Lin EY, Wang Y, Pixley F, Stanley ER, Graf T, Pollard JW, Segall J, Condeelis J.** A paracrine loop between tumor cells and macrophages is required for tumor cell migration in mammary tumors. *Cancer Res* 64: 7022–7029, 2004. doi:10.1158/0008-5472.CAN-04-1449.
63. **Xing M, Peterman MC, Davis RL, Oegema K, Shiau AK, Field SJ.** GOLPH3 drives cell migration by promoting Golgi reorientation and directional trafficking to the leading edge. *Mol Biol Cell* 27: 3828–3840, 2016. doi:10.1091/mbc.E16-01-0005.
64. **Yachida S, Iacobuzio-Donahue CA.** Evolution and dynamics of pancreatic cancer progression. *Oncogene* 32: 5253–5260, 2013. doi:10.1038/onc.2013.29.
65. **Yang AD, Camp ER, Fan F, Shen L, Gray MJ, Liu W, Somcio R, Bauer TW, Wu Y, Hicklin DJ, Ellis LM.** Vascular endothelial growth factor receptor-1 activation mediates epithelial to mesenchymal transition in human pancreatic carcinoma cells. *Cancer Res* 66: 46–51, 2006. doi:10.1158/0008-5472.CAN-05-3086.
66. **Yin Y, Grabowska AM, Clarke PA, Whelband E, Robinson K, Argent RH, Tobias A, Kumari R, Atherton JC, Watson SA.** *Helicobacter pylori* potentiates epithelial:mesenchymal transition in gastric cancer: links to soluble HB-EGF, gastrin and matrix metalloproteinase-7. *Gut* 59: 1037–1045, 2010. doi:10.1136/gut.2009.199794.
67. **Zeng G, Germinaro M, Micsenyi A, Monga NK, Bell A, Sood A, Malhotra V, Sood N, Midda V, Monga DK, Kokkinakis DM, Monga SP.** Aberrant Wnt/beta-catenin signaling in pancreatic adenocarcinoma. *Neoplasia* 8: 279–289, 2006. doi:10.1593/neo.05607.
68. **Zheng L, Xue J, Jaffee EM, Habtezion A.** Role of immune cells and immune-based therapies in pancreatitis and pancreatic ductal adenocarcinoma. *Gastroenterology* 144: 1230–1240, 2013. doi:10.1053/j.gastro.2012.12.042.
69. **Zhou BP, Deng J, Xia W, Xu J, Li YM, Gunduz M, Hung MC.** Dual regulation of Snail by GSK-3beta-mediated phosphorylation in control of epithelial-mesenchymal transition. *Nat Cell Biol* 6: 931–940, 2004. doi:10.1038/ncb1173.
70. **Zhuang K, Yan Y, Zhang X, Zhang J, Zhang L, Han K.** Gastrin promotes the metastasis of gastric carcinoma through the beta-catenin/TCF-4 pathway. *Oncol Rep* 36: 1369–1376, 2016. doi:10.3892/or.2016.4943.